

Differential diagnosis between acinic cell carcinoma and pleomorphic adenoma using the quantitative parameters of contrast-enhanced ultrasound

J.-M. GUO¹, Q. CHEN², H. WU², L.-T. FENG², J. CHEN², W.-B. CHAO²

¹Department of Ultrasound Diagnosis, The Sixth People's Hospital of Chengdu, Chengdu, Sichuan, P.R. China

²Department of Ultrasound Diagnosis, Sichuan Provincial People's Hospital, Chengdu, Sichuan, P.R. China

Abstract. – **OBJECTIVE:** To investigate the value of differential diagnosis between acinic cell carcinoma (ACC) and pleomorphic adenoma (PA) using the quantitative parameters of contrast-enhanced ultrasound (CEUS).

PATIENTS AND METHODS: Twenty-two ACC and 98 PA were retrospectively analyzed. These patients had been examined via routine pre-surgical two-dimensional ultrasound and CEUS. The examination results were confirmed by biopsy pathology. Contrast 4.0 imaging analysis software was applied to obtain the maximum intensity (PEAK), time to peak (TTP), regional blood volume (RBV), regional blood flow (RBF), maximum signal intensity (SI_{max}) and mean signal intensity (SI_{mean}) through quantitative analysis. The differences between ACC and PA were compared regarding the conventional ultrasound images and the quantitative parameters of CEUS. ROC curves were drawn to evaluate the diagnostic value of these parameters.

RESULTS: There were no statistically significant differences between salivary gland ACC and PA in the manifestations of conventional two-dimensional ultrasound examination regarding morphology, internal echo and the boundary ($p > 0.05$). However, there were significant differences in PEAK, RBV, RBF, SI_{max} and SI_{mean} between ACC and PA ($p < 0.05$). Additionally, the five quantitative parameters of CEUS were all highly accurate diagnostic indicators. The maximum area under the curve of each parameter was 0.888, sensitivity 72.6%, specificity 90.9% and accuracy 81.8%.

CONCLUSIONS: The quantitative parameters of CEUS are helpful for differentially diagnosing salivary ACC and PA.

Key Words:

Acinic cell carcinoma, Pleomorphic adenoma, Contrast-enhanced ultrasound, Quantitative parameters, Differential diagnosis.

Introduction

The histological types and cell morphology of acinic cell carcinoma (ACC) are complex and diverse and is similar to pleomorphic adenoma (PA) of the salivary glands. ACC is a rare low-grade malignant tumour of the salivary gland that is highly invasive and prone to recurrence and metastasis. PA is the most common benign epithelial neoplasm, with low risks in terms of long-term recurrence and secondary malignant transformation. Long-term recurrence risks were low, and secondary malignant transformation risks were very low¹. Therefore, it is of great clinical significance to correctly identify these two tumours for disease treatment and prognostic evaluation. Most studies have found that primary ACC appears as benign tumors on ordinary two-dimensional ultrasound, ordinary CT, MR. It is difficult to differentiate ACC from benign tumors, especially from PA^{2,3}. However, contrast-enhanced ultrasound (CEUS) can be used to differentiate them, which provides a more objective quantitative diagnostic basis for clinical diagnosis.

Patients and Methods

Patients

A retrospective analysis was conducted among 22 cases of salivary ACC (14 females and 8 males), and 98 cases of PA (42 females and 56 males). These patients were admitted to our Hospital from April 2008 to May 2017. The ACC patients aged 12 to 64 years (mean 49.9 ± 15.9

years). The maximum diameter of tumors was 1.5 to 7.8 cm (3.6 ± 1.8 cm). The ACC cases included 16 cases of parotid glands, 2 cases of submandibular glands, 4 cases of salivary glands, 1 case of lymph node metastasis and 1 case of recurrence. The PA patients aged from 13 to 74 years (mean, 51.6 ± 18.2 years). The maximum diameter of tumors was 1.0 to 7.8 cm (2.7 ± 1.5 cm). The PA cases included 62 cases of parotid glands, 28 cases of submandibular glands, 8 cases of salivary glands, no cases of lymph node metastasis and 1 case of recurrence. The patient was treated with a salivary gland mass. Routine ultrasound and contrast-enhanced ultrasound (CEUS) were performed on all cases before surgery, with pathological confirmation after surgery. None of the patients had serious heart, lung or blood diseases, or salivary gland diffusing diseases. This study was approved by the Ethics Committee of our Hospital. Written informed consent was obtained from each subject before the study. All procedures in this study were in compliance with the Declaration of Helsinki⁴.

Instruments and Methods

MyLab90 (Esaote, Genoa, Italy) and GE E9 (GE Healthcare, Austria) were employed. Linear array transducer LA523 and L9 were used with a center frequency of 4 to 13 MHz, and linear array transducers LA522 was used with a center frequency of 3 to 9 MHz. The contrast agent SonoVue; (Bracco, Milan, Italy) was applied. The Qontrast 4.0 (Bracco, Milan, Italy), a specific quantitative perfusion analysis software, was used. Firstly, the salivary gland mass was scanned using conventional ultrasound, with transverse, longitudinal and oblique images to select the appropriate ultrasonic section, displaying the com-

plete salivary gland mass and the adjacent normal tissue. Contrast Turned Imaging (CnTI) was fixed as follows: frequency (7 MHz), power (3%), gray scale (46%), sound pressure (45 kPa) and mechanical index (0.05). In accordance with the manual, 4.8 ml of SonoVue was quickly injected into the cubital vein, followed by 5 ml of a 0.9 % normal saline flush. The timer was started when the bolus was injected. The 120-180 s dynamic image was recorded and saved on the hard drive of the ultrasound machine for later documentation and analysis.

Comparative Analysis of Ultrasonic Images

By playing back previously stored two-dimensional static images (Figure 1), the PA and ACC masses were examined in terms of the following aspects: (1) the shapes of the salivary gland masses, either regular or irregular involving lobulation; (2) internal echoes of the tumours, classified as either homogeneous or heterogeneous involving the interior content of the cyst; (3) the tumour margin, either well-defined or not.

Qontrast 4.0 was used offsite for CEUS quantitative analysis of the salivary gland masses. First, the analysis area was defined by manual delineation of the full lesion area. Then the highly perfused area within the lesion was defined as ROI (region of interest) by pseudo-colour simulation automatically generated by Qontrast 4.0 (red in the figures indicates highly perfused areas or rapidly peaking areas in the mass, whereas blue shows the poorly perfused areas). The ROI was not close to perfusion defect area. The sample area in calcified lesion was usually about 0.1 cm^2 in volume (Figure 2). This ROI is automatically analysed by Qontrast

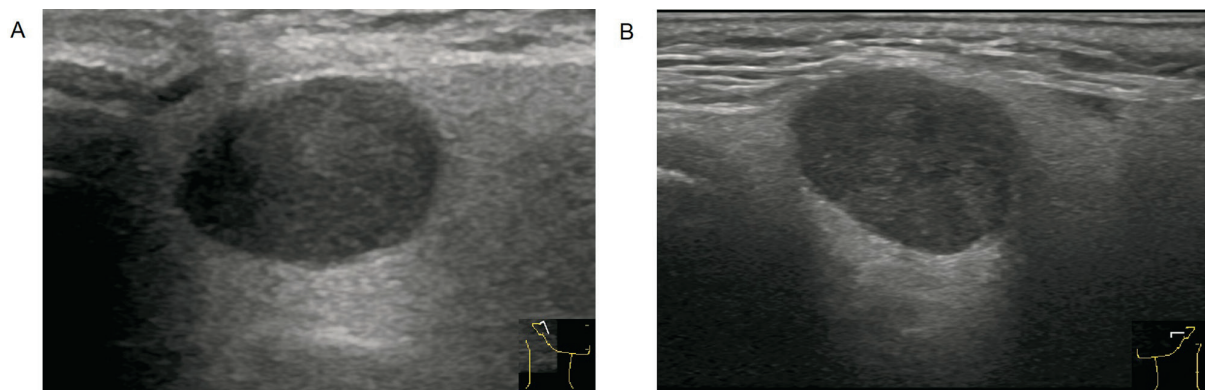


Figure 1. Two-dimensional static images ACC (A), PA (B).

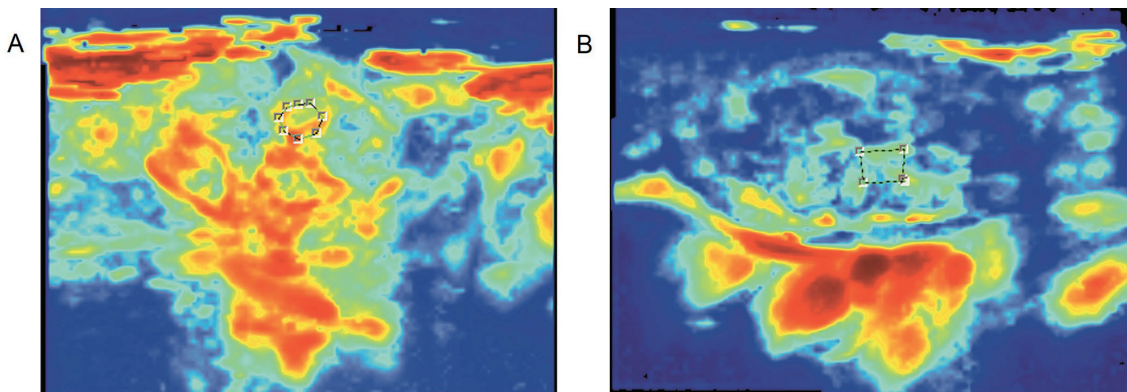


Figure 2. Pseudocolour simulation and ROI Area of ACC (A), Pseudocolour simulation and ROI Area of PA (B).

4.0 to generate a gamma-varied time-intensity curve. The following mean perfusion parameters can be acquired from the curve: PEAK (maximum intensity of the US signal), TTP (time to peak), RBV (regional blood flow), RBF (regional blood flow), SI_{max} (maximum signal intensity), and SI_{mean} (mean signal intensity) (Figure 3).

Statistical Analysis

SPSS v20.0 (IBM Corp., Armonk, NY, USA) statistical software was employed to analyse the data. Comparisons of counting data were performed using the χ^2 test (Fisher's exact probability test was adopted when the number of cells with $T < 1$ or $1 \leq T < 5$ exceeded 1/5 of the total number of cells). The measurement data were expressed as the standard deviation of the sample mean ($\bar{X} \pm S$). For comparison of the tumour parameters, t -tests (homogeneity of variance) were performed in a group of independent samples, with the test level set at 0.05. A difference was considered statistically significant when $p < 0.05$. ROC curve analysis of the quantitative parameters of CEUS alone and combined was adopted for the differential diagnosis of salivary gland ACC and PA; there was statistical significance when it comes to $p < 0.05$.

Results

Comparison Between Salivary ACC and PA Using Ultrasonic Two-Dimensional Examination

The morphology, boundary and internal echo of salivary gland ACC and PA were compared by conventional two-dimensional ultrasonography. No significant differences were found ($p > 0.05$) (Table I).

Comparison of CEUS Quantitative Parameters Between Salivary Gland ACC and PA

The quantitative parameters of the CEUS time-intensity curves of salivary gland ACC and PA were compared using independent sample t -tests. Salivary gland ACC had higher SI_{mean} , PEAK, RBV, RBF, SI_{max} and SI_{mean} compared with those of PA. There were significant differences in PEAK, RBV, RBF, SI_{max} and SI_{mean} ($p < 0.05$) under the fitting curve between salivary gland ACC and PA.

The TTP of salivary gland ACC was significantly shorter than that of PA ($p < 0.05$). Conversely, no significant difference was found for MTT between ACC and PA ($p > 0.05$) (Table II).

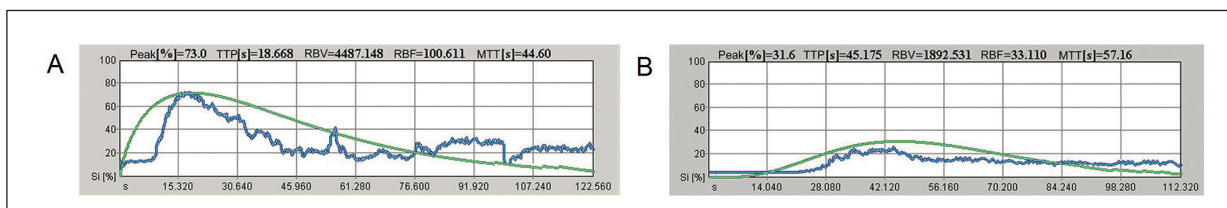


Figure 3. CEUS time-intensity curve of ACC and its quantitative parameters (A), PA and its Quantitative parameters (B).

Table I. The Contrast between salivary ACC and PA in Ultrasonic two-dimensional examination.

Groups (cases. n)	Shape		Border		Internal echo	
	regular	irregular	clear	unclear	even	uneven
ACC (22)	14	8	17	5	12	10
PA (98)	74	24	85	13	68	30
χ^2	1.295		1.262		1.781	
p	0.255		0.261		0.182	

*The difference of ACC and PA was not statistically significant ($p>0.05$).

Table II. Comparison of CEUS quantitative parameters between salivary gland ACC and PA ($\bar{x}\pm S$).

Quantitative parameters	ACC	PA	t	p
PEAK	56.73±11.31	39.59±13.71	-5.45	0.000
TTP	25.72±8.42	41.77±22.22	3.32	0.001
RBV	3791.13±1721.61	2928.06±1809.70	-2.03	0.044
RBF	72.10±19.49	49.13±24.92	-4.04	0.000
MTT	46.97±13.76	56.86±23.74	1.88	0.63
SI _{max}	68.64±16.45	56.22±14.53	-3.72	0.000
SI _{mean}	55.73±10.59	43.94±16.45	-3.21	0.002

*PEAK, TTP, RBV, RBF, SI_{max}, SI_{mean} $p<0.05$; MTT, $p>0.05$

The Differential Diagnostic Performance of Salivary Gland ACC and PA Based on ROC Curve Analysis of Quantitative CEUS Parameters Alone and in Combination

Because there were significant differences in the PEAK, TTP, RBV, RBF, SI_{max} and SI_{mean} of the fitted curve between salivary gland ACC and PA, the five quantitative parameters could potentially serve as diagnostic indices alone or together (Figure 4).

Table III shows that all the diagnostic indices were highly accurate. The maximum AUC of the individual quantitative parameters was 0.824, sensitivity was 66.3%, specificity was 86.6% and accuracy was 76.4%. The maximum AUC of the combined quantitative parameters was 0.888, sensitivity was 72.6%, specificity was 90.9% and accuracy was 81.8%.

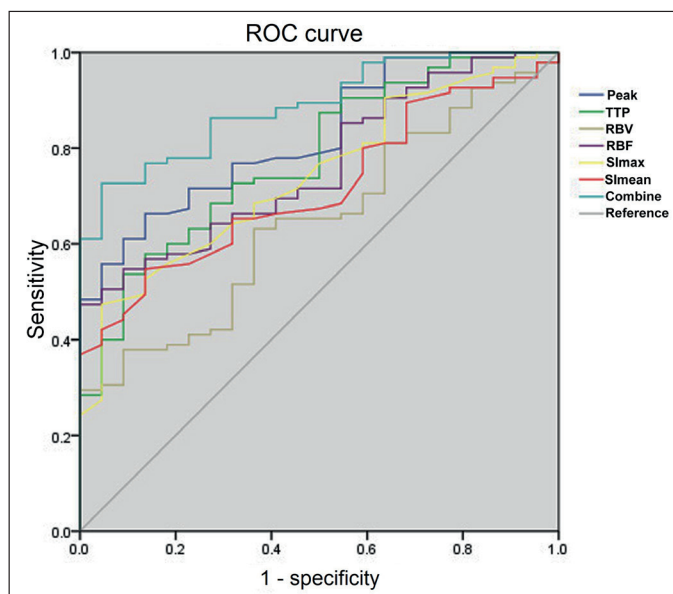


Figure 4. The ROC curve from quantitative CEUS parameters of ACC and PA: PEAK, TTP, RBV, RBF, SI_{max}, SI_{mean} and their combination ($p<0.05$).

Table III. The differential diagnostic performance of salivary gland ACC and PA based on ROC curve analysis of quantitative CEUS parameters alone and in combination.

Method	Area under ROC curve (95% Confidence Inter-val)	Sensitivity (%)	Specificity (%)	Accuracy (%)	<i>p</i>
PEAK	0.824	66.3%	86.4%	76.4%	0.000
TTP	0.779	72.6%	68.2%	70.4%	0.000
RBV	0.646	63.2%	63.6%	63.4%	0.033
RBF	0.763	54.7%	90.9%	72.8%	0.000
SI _{max}	0.741	55.8%	88.8%	72.0%	0.000
SI _{mean}	0.716	54.7%	86.4%	70.1%	0.002
Combined	0.888	72.6%	90.9%	81.8%	0.000

Discussion

PA is one of the most common benign tumours in the salivary gland, accounting for 45.5% of all salivary gland tumours, about 80% of benign salivary gland tumours and 60%-70% of primary parotid tumours^{5,6}. ACC is a relatively rare malignancy of ductal cell origin that represents 6-10% of the total malignant tumors of these glands. It is considered to be the third most common epithelial malignancy of the salivary glands in adults, and the second common in children. The ACC originates in the parotid in 81-98% of the cases, in the submandibular glands in 11% of the cases, and in the minor salivary glands in 3-12% of the cases. ACC is a relatively rare malignancy of ductal cell origin that accounts for 6%-10% of the total malignant tumours of these glands. It is the third and second most common epithelial malignancy of the salivary glands respectively in adults and children. ACC originates in the parotid glands in 81%-98% of cases, the submandibular glands in 11% of cases and the minor salivary glands in 3%-12% of cases⁷. However, most clinicians still associate ACC to a good prognosis. Recent studies increase our awareness of the propensity of this tumor for lymphatic invasion and distant metastases. It develops in a protracted and unpredictable clinical course. Indeed, there were distant metastases to the lungs, pleura, brain, peritoneum, paraaortic, paratracheal, and mediastinal lymph nodes, as well as cutaneous metastases. Most clinicians believe that ACC has a good prognosis. However, distant metastasis may occur in the lungs, pleura, brain, peritoneum, para-aorta, pneumotracheal and mediastinal lymph nodes, and the skin⁸. Therefore, it is very important to distinguish ACC from benign PA. Conventional two-dimensional high-frequency ultrasonography shows that malignant masses are irregular in shape,

indistinct in boundary and heterogeneous and hypoechoic. Conversely, benign masses are characterised by regular morphology, clear boundaries and are homogeneous and hypoechoic. However, in this study, the majority of the ACC were regular in morphology (65%), had clear boundaries (80%) and were heterogeneous and hypoechoic (55%). Most of the PA were regular in morphology (76%), had well-defined boundaries (69%) and were inhomogeneous and hypoechoic (87%). No statistically significant differences could be seen when using conventional ultrasonography in morphology, internal echo or boundary between salivary gland ACC and PA ($p > 0.05$) (Table I). Therefore, routine ultrasonography of lesion morphology, boundary and internal echogenicity cannot differentiate salivary gland ACC from PA. Our results are consistent with those of previous studies^{2,3,9,10}. Both morphologies are regular or partially lobulated, with clear boundaries (Figure 1).

This may be due to the slow growth and long course of PA and ACC. PA showed expansive growth, while ACC showed invasive growth. In the early and middle stages of growth, the tumour cells only infiltrated the capsule. The internal echo for both tumours was uneven, which may be related to the complex pathological composition of these tumours. ACC is composed of acinic cells, non-specific glandular cells, leap tube sample cells, cavitation cells and transparent sample cells. ACC pushes the salivary gland tissue around to form pseudocapsule, both the basophilic cells and transparent cell were laid out in entity shape, less interstitial². PA is composed of the epithelial cells of the tumour and myxoid and chondroid tissue, and is characterised by membrane integrity, epithelial cell nests and myxoid matrix interval¹¹ (Figure 5). ACC is formed by acinic cells describing a pattern with little stroma visible. In well differentiated tumors,

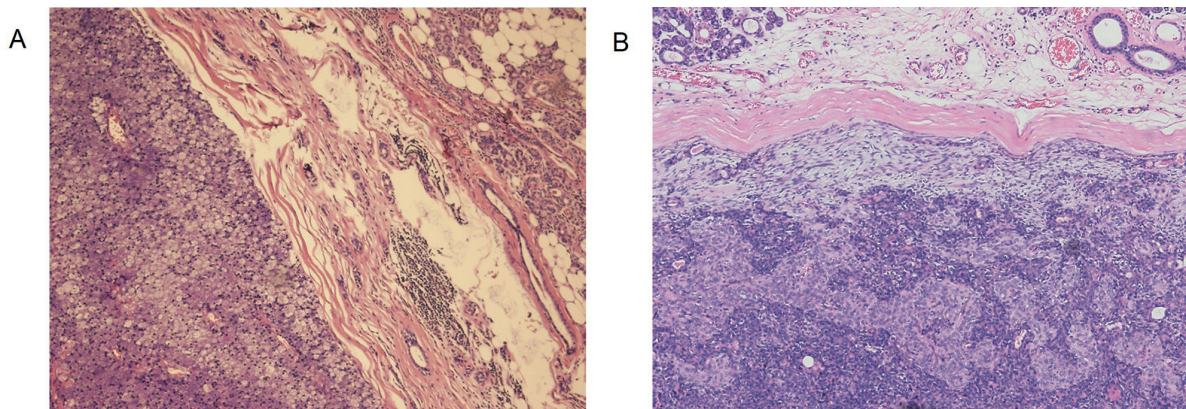


Figure 5. ACC: pushes out surrounding salivary gland tissue to form a pseudocapsule, Basophils and clear cells in Solid arrangement with less Interstitial (**A**), PA: complete capsule, Epithelial cell nest and Myxoid matrix in Interval arrangement (**B**) (200X).

the neoplasia has innocuous appearance because of the similarity between the normal parotid tissue and the neoplastic tissue in both morphological and biochemical aspects. That makes it more difficult to diagnose. In well-differentiated tumours, the morphological and biochemical similarities between normal parotid tissue and tumour tissue increase the difficulty of diagnosis¹².

Previous research^{2,6} has examined ACC and PA using contrast-enhanced computed tomography (CECT) and found little or no evident enhancement in the early stage of PA. There was evident enhancement in the delayed stage, and evident enhancement was also observed during both the early and delayed stages of ACC¹³⁻¹⁵. Thus, the degree of contrast enhancement can be used to differentiate ACC and PA. In our study, CEUS was employed to observe the tumours. The ultrasound contrast agent was injected rapidly via the elbow superficial vein, which can effectively enhance the lesion blood vessel contrast, with more abundant distribution into the small blood vessels and blood capillaries. The blood flow features of the capillary network can be seen. Therefore, it

remarkably improves the resolution of ultrasonic diagnosis, accuracy, sensitivity and specificity.

The TTP of salivary gland ACC was significantly shorter than that of PA. Contrast enhancement was faster in ACC than that in PA, and this difference was statistically significant ($p < 0.05$) (Figure 6). Li et al² reported that the degree of contrast enhancement in CECT could be used to distinguish ACC and PA. The degree of enhancement in ultrasound showed the PEAK, RBV, RBF, SI_{max} and SI_{mean} of the tumour after contrast enhancement. In this study, the PEAK, RBV, RBF, SI_{max} and SI_{mean} were significantly higher after ultrasound contrast enhancement in salivary gland ACC than those in PA ($p < 0.05$) (Table II) (Figure 7). The CEUS results were consistent with the above CT enhancement results, indicating that the difference in the degree of CEUS enhancement can also be used to distinguish ACC from PA.

The reason for the different intensities of the two types of adenomas may be that PA is derived from benign epithelial-derived tumours with slow growth and low vascular distribution¹⁶. However, malignant tumours show invasive growth and are

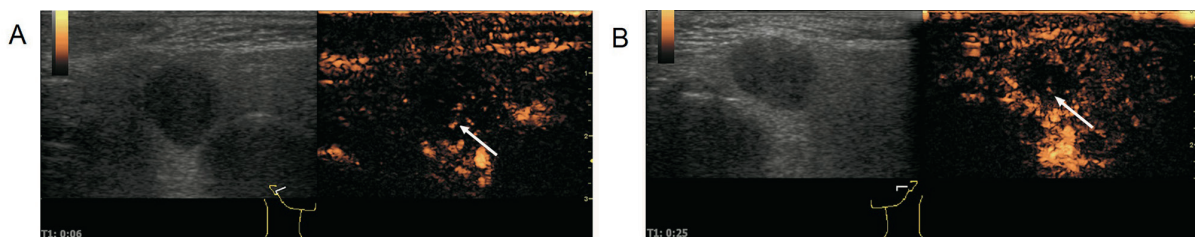


Figure 6. ACC of the parotid gland (The arrow shows the contrast agent began to strengthen 6 s after injection) (**A**), PA of the parotid gland (The arrow shows the contrast agent began to strengthen 25 s after injection) (**B**), contrast enhancement was faster in ACC than that in PA.

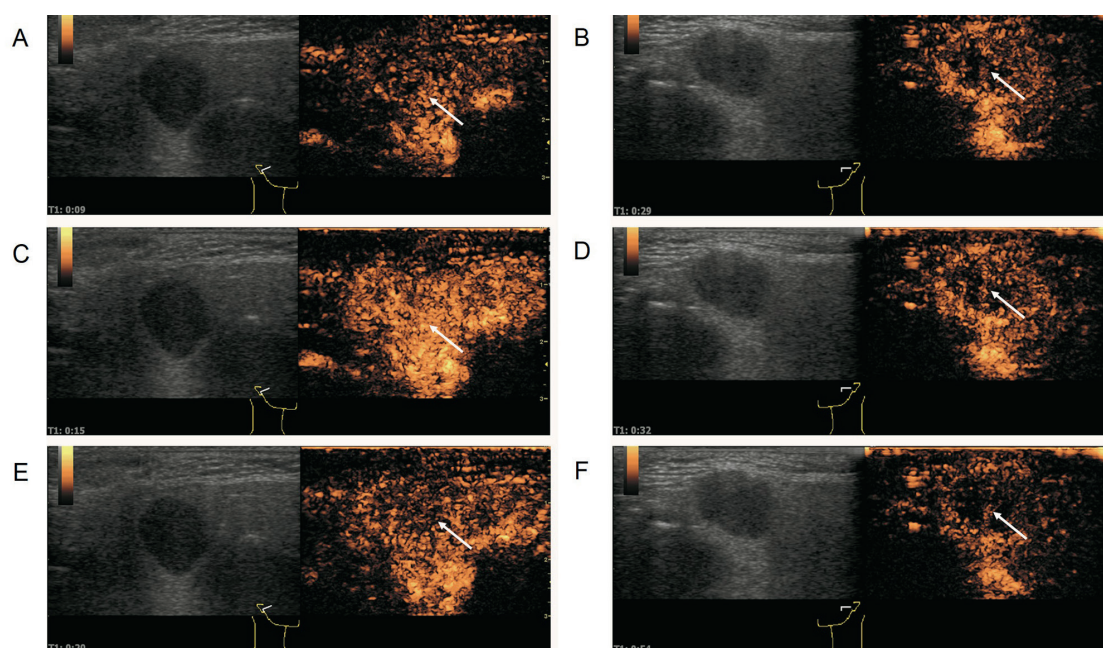


Figure 7. ACC of the parotid gland (The arrow shows the contrast agent 9 s,15 s,20 s after the injection of contrast agent, TTP:15 s) (A,C,E), PA of the parotid gland (29 s,32 s,54 s after the injection of contrast agent, TTP: 32 s) (B,D,F).

induced by various angiogenic factors, with increased numbers of new blood vessels, expanded lumen and abundant anastomosis to form arteriovenous fistula¹⁷. Therefore, the amount of contrast agent entering PA was low, and the contrast agent passed through the lesion slowly. More contrast agent entered ACC, and the contrast agent passed through ACC quickly. There were significant differences in PEAK, TTP, RBV, RBF, SI_{max} and SI_{mean} between salivary gland ACC and PA. These five quantitative parameters could potentially serve as diagnostic indices using their ROC curves alone or together (Figure 4).

Our results indicate that the diagnostic indices of the five quantitative parameters had high accuracy. A single quantitative diagnosis index (AUC) showed that: the maximum was 0.824, the sensitivity 66.3%, the specificity 86.6% and the accuracy 76.4%; the joint diagnosis index AUC showed that: the maximum was 0.888, the sensitivity 72.6%, the specificity 90.9% and the accuracy 81.8%. Therefore, the sensitivity, specificity and accuracy of the five combined quantitative parameters were the highest (Table III). It is difficult to differentiate ACC and PA by ordinary ultrasound, CT and MR, but we can make differential diagnosis by ceUS and quantitative parameters of ceUS, so ceUS can provide a more objective and quantitative basis for clinical diagnosis.

Conclusions

Shortly, it is difficult to distinguish between ACC and PA using conventional ultrasonography. However, the differences in the findings of CEUS and its quantitative parameters can be used to identify ACC and PA, and this method has many potential clinical applications.

Conflict of Interests

The authors declare that they have no conflict of interest.

References

- 1) Valstar MH, de Ridder M, van den Broek EC, Stuiver MM, van Dijk BAC, van Velthuisen MLF, Balm AJM, Smeele LE. Salivary gland pleomorphic adenoma in the Netherlands: A nationwide observational study of primary tumor incidence, malignant transformation, recurrence, and risk factors for recurrence. *Oral Oncol* 2018; 66: 93-99.
- 2) Li J, Gong X, Xiong P, Xu Q, Liu Y, Chen Y, Tian Z. Ultrasound and computed tomography features of primary acinic cell carcinoma in the parotid gland: a retrospective study. *Eur J Radiol* 2014; 83: 1152-1156.

- 3) Kashiwagi N, Nakatsuka SI, Murakami T, Enoki E, Yamamoto K, Nakanishi K, Chikugo T, Ku-risu Y, Kimura M, Hyodo T, Tsukabe A, Kakigi T, Tomita Y, Ishii K, Narumi Y, Yagyu Y, To-miyama N. MR imaging features of mmary analogue secretory carcinoma and acinic cell carcinoma of the salivary gland: a preliminary report. *Dentomaxillofac Radiol* 2018; 47: 20170218.
- 4) General Assembly of the World Medical A. World Medical Association Declaration of Helsinki: Ethical principles for medical research involving human subjects. *J Am Coll Dent* 2014; 81: 14-18.
- 5) Thielker J, Weise A, Othman MAK, Liehr, T. Molecular cytogenetic pilot study on pleomorphic adenomas of salivary glands. *Oncol Lett* 2020; 19: 1125-1130.
- 6) Jung YJ, Han M, Ha EJ, Choi JW. Differentiation of salivary gland tumors through tumor heterogeneity: a comparison between pleomorphic adenoma and Warthin tumor using CT texture analysis. *Neuroradiology* 2020; 62: 1451-1458.
- 7) Buhaş CL, Roşca E, Muţiu G, Venter AC, Buhaş BA, Couţi R, Ciobanu CF, Roşca DM. Acinic cell carcinoma of minor salivary glands—case report. *Rom J Morphol Embryol* 2017; 58: 1003-1007.
- 8) Vander Poorten V, Triantafyllou A, Thompson LD, Bishop J, Hauben E, Hunt J, Skalova A, Stenman G, Takes RP, Gnepp DR, Hellquist H, Wenig B, Bell D, Rinaldo A, Ferlito A. Salivary acinic cell carcinoma: reappraisal and update. *Eur Arch Otorhinolaryngol* 2016; 273: 3511-3531.
- 9) Wu S, Liu G, Chen R, Guan Y. Role of ultrasound in the assessment of benignity and malignancy of parotid masses. *Dentomaxillofac Radiol* 2012; 41:131-135.
- 10) Bialek EJ, Jakubowski W, Zajkowski P, Szopinski KT, Osmolski A. US of the major salivary glands: anatomy and spatial relationships, pathologic conditions, and pitfalls. *Radiographics* 2006; 26: 745-763.
- 11) Seifert G, Brocheriou C, Cardesa A, Eveson JW. WHO International Histological Classification of Tumours Tentative Histological Classification of Salivary Gland Tumours. *Pathol Res Pract* 1990; 186: 555-581.
- 12) Rosero DS, Alvarez R, Gambó P, Alastuey M, Valero A, Torrecilla N, Roche AB, Simón S. Acinic Cell Carcinoma of the Parotid Gland with Four Morphological Features. *Iran J athol* 2016; 11: 181-185.
- 13) Yerli H, Teksam M, Aydin E, Coskun M, Ozdemir H, Agildere AM. Basal celladenoma of the parotid gland: dynamic CT and MRI findings. *Br J Radiol* 2005; 78: 642–645.
- 14) Lev MH, Khanduja K, Morris PP, Curtin HD. Parotid pleomorphic adenomas: delayed CT enhancement. *AJNR Am J Neuroradiol* 1998; 19: 1835–1839.
- 15) Choi DS, Na DG, Byun HS, Ko YH, Kim CK, Cho JM, Lee HK. Salivary gland tumors: evaluation with two-phase helical CT. *Radiology* 2000; 214: 231–236.
- 16) Fisher DE, Baltzer P, Malich A, Wurdinger S, Freesmeyer MG, Marx C, Kaiser WA. Is the blooming sign a Promising additional tool to determine malignancy in MR mammography. *Eur Radiol* 2004; 14: 394-401.
- 17) Xiong YL, Hao J, Wang H, Guo YX. Application of real - time contrast enhanced mode of gray - scale ultrasound in the differential diagnosis of thyroid nodules. *Chinese Journal of Medical Ultrasound* 2011; 27: 980-983.